

## Evaporating droplets: comparisons between DNS and modelling

Benjamin Duret\*, Mansour Al Qubeissi, Sergei Sazhin, Cyril Crua

Sir Harry Ricardo Laboratories, School of Computing, Engineering and Mathematics, University of Brighton, Lewes Road, Brighton BN2 4GJ, United Kingdom

\*Corresponding author: b.duret@brighton.ac.uk

### Abstract

This study focuses on preliminary analysis of the heating and evaporation processes in a spherical moving droplet using Direct Numerical Simulation (DNS) and simplified modelling approaches. DNS of two-phase flows is used to obtain detailed information about heat and mass transfer at the interface. The DNS results are compared with the results predicted by the modelling approach, based on the analytical solution to the heat transfer equation inside the droplet. The latter approach takes into account the finite thermal conductivity and recirculation inside droplets using the effective thermal conductivity (ETC) model. The ETC model has been widely used by the scientific community since it was originally developed by Abramzon and Sirignano more than 25 years ago, although its range of applicability has never been rigorously investigated. The comparison between DNS and modelling results is performed for a wide range of Peclet numbers in the analysis of transient heating of droplets without evaporation. A DNS database has been created. DNS results are shown to be rather different from the modelling results when the model is used for relatively low Peclet numbers. These results, however, turned out to be in good agreement for relatively high Peclet numbers.

### Introduction

In most CFD codes, sprays are modelled using the Lagrangian techniques: point particles are used to represent the location of droplets inside sprays, each droplet has its own characteristics (e.g. velocity, diameter). This analysis is based on the hypothesis that droplets remain spherical [1]. This hypothesis, however, is not always consistent with experimental observations: liquid structures can be widely deformed.

To investigate the deformation of droplets, and liquid structures of any shape, one can use an interface tracking method [2,3]. This method is very attractive as it allows the interface to be directly resolved. In this context, incompressible Navier-Stokes equations are solved directly and jump conditions (change in density and viscosity across the interface) are taken into account using advanced numerical methods. This kind of simulation is called Direct Numerical Simulation (DNS) of two-phase flows. ARCHER (in-house code) has been developed to perform DNS of the above-mentioned two-phase flows. This code has been widely used and was one of the first to be applied to perform DNS of Diesel injection [2]. Phase change has also been recently implemented into this code, following the Tanguy et al. method [3]. A comparison between the primary atomisation model ELSA (Eulerian-Lagrangian Spray Atomization model) and DNS has been performed to evaluate the ELSA model [4]. The main objective of this work is to perform a preliminary comparison between modelling and DNS results.

The Abramzon-Sirignano modelling approach [5] is used in our analysis. This approach is based on the application of the effective thermal conductivity (ETC) model to take into account the effects of finite thermal conductivity and vortices inside moving droplets on droplet heating and evaporation. This model is based on the assumption that the droplet surface temperature is uniform, although it can change with time. The range of applicability of this assumption is not at first evident.

### Numerical methods

Numerical methods of handling phase change and interface tracking are based on the method suggested by Tanguy et al. [3]. A level set function is used to capture the interface and the ghost fluid method (GFM) is applied to track sharp discontinuities at the interface (see [2,3,4] for further details). The level set function is defined as the signed distance between any point of the domain and the interface. The equation describing the motion of the reactive interface reads:

$$\frac{\partial G}{\partial t} + \mathbf{V} \cdot \nabla G = 0, \quad (1)$$

where  $G$  is the level set function,  $t$  time and  $\mathbf{V}$  the velocity vector. Spatial derivatives are solved with a fifth-order WENO scheme and a third-order Runge-Kutta scheme is used for the temporal integration. The same approach is applied to all

equations presented in this section, except for the diffusion terms, the analysis of which is based on a second-order central finite difference scheme.

The level set method is coupled with a projection method to carry out the direct numerical simulation of the incompressible Navier Stokes equation:

$$\frac{\partial \mathbf{V}}{\partial t} + (\mathbf{V} \cdot \nabla) \mathbf{V} = -\frac{\nabla p}{\rho} + \frac{1}{\rho} \nabla \cdot (2\mu \mathbf{D}) + \mathbf{f} + \frac{1}{\rho} \sigma \kappa \delta(G) \mathbf{n} \quad , \quad (2)$$

where  $p$  is the fluid pressure,  $\rho$  density,  $\mathbf{f}$  external forces (e.g. gravity),  $\mu$  dynamic viscosity, and  $\mathbf{D}$  viscous deformation tensor. At the interface, the surface tension force is taken into account using the Dirac function  $\delta(G)$ :  $\sigma$  surface tension,  $\mathbf{n}$  normal unit vector,  $\kappa$  curvature computed from the level set function  $G$ .

To take into account heat and mass transfer, additional equations such as energy and species equations need to be solved. Assuming that the flow is incompressible, the following set of equations has been implemented into the code:

$$\frac{\partial h_s}{\partial t} + \mathbf{V} \cdot \nabla h_s = \frac{1}{\rho} \nabla \cdot (\lambda \nabla T) \quad (3)$$

$$\frac{\partial Y_v}{\partial t} + \mathbf{V} \cdot \nabla Y_v = \nabla \cdot (D_m \nabla Y_v) \quad , \quad (4)$$

where  $\lambda$  is thermal conductivity,  $h_s$  is sensible enthalpy,  $D_m$  is the diffusion coefficient and  $Y_v$  the vapour mass fraction. Fluid properties ( $c_p$ ,  $\rho$ ,  $\lambda$  and  $D_m$ ) are not affected by temperature, but are discontinuous across the interface. To the best of the authors' knowledge there are no evaporating two-phase flow DNS studies in the literature which take into account the temperature dependence of physical properties such as density and viscosity. Taking this dependence into account would increase the overall complexity of the analysis and would require considerable modification of the numerical method.

Firstly, we restrict our study to the heating of droplets; phase change is not considered. In this case, species equations are not solved and the energy jump condition simplifies to:

$$[\lambda \nabla T \cdot \mathbf{n}] = 0 \quad (5)$$

The ghost fluid method is used to take into account this jump condition. Sensible enthalpy is discontinuous across the interface. As mentioned by Tanguy et al. [3], Aslam extrapolation [6] can be used to estimate spatial derivatives for discontinuous variables. The same technique is applied for the enthalpy.

Since we ignore phase change and Stefan flow, velocities remain continuous at the interface and a standard projection method can be used for their estimation.

Validation of the numerical method (including evaporating liquid-gas flows) has been the subject of previous studies [7,8], and will not be discussed in this work.

Our method could be used to study evaporating deformed droplets. Keeping in mind, however, that DNS of evaporative two-phase flows is at least twice as CPU expensive as that of the two-phase flows without evaporation, we ignored the latter process for the time being.

## Modelling

The analysis of droplet heating, taking into account finite thermal conductivity inside droplets and recirculation within them is based on the following equation for the temperature [1,9]:

$$\frac{\partial T}{\partial t} = \frac{\lambda_{eff}}{\rho_l c_{pl}} \left( \frac{\partial^2 T}{\partial R^2} + \frac{2}{R} \frac{\partial T}{\partial R} \right) + P(R) \quad (6)$$

where  $\lambda_{eff}$  is the effective thermal conductivity (ETC) defined as  $\lambda_{eff} = \lambda_l \chi$ ,  $\chi$  is the correction factor to take into account the effect of recirculation inside droplets; it varies from about 1 (at droplet Peclet number <10) to 2.72 (at droplet Peclet number >500) [5],  $P(R)$  takes into account droplet heating by external thermal radiation (ignored in our analysis),  $R$  is the distance from the centre of the droplet.

The solution to Equation (6), subject to conventional boundary and initial conditions for  $h=\text{const}$ , can be presented as [1,9]:

$$T = T_{eff} + \frac{R_d}{R} \sum_{n=1}^{\infty} \left\{ \left[ q_n - \frac{\sin \lambda_n \mu_0(0)}{\lambda_n^2 \|V_n\|^2} \right] \exp(-\kappa_0 \lambda_n^2 t) - \frac{\sin \lambda_n}{\lambda_n^2 \|V_n\|^2} \int_0^1 \frac{d\mu_0(\tau)}{d\tau} \exp[-\kappa_0 \lambda_n^2 (t-\tau)] d\tau \right\} \sin\left(\frac{\lambda_n R}{R_d}\right) + \frac{R_d}{R} \sum_{n=1}^{\infty} \frac{p_n}{\kappa_0 \lambda_n^2} [1 - \exp(-\kappa_0 \lambda_n^2 t)] \sin\left(\frac{\lambda_n R}{R_d}\right), \quad (7)$$

where

$$\mu_0 = \frac{hT_{eff}(t)R_d}{k_l}, q_n = \frac{1}{\|V_n\|^2} \int_0^1 \bar{T} V_n(R) d(R/R_d), \quad T_{d0} \text{ is the droplet initial temperature distribution,}$$

$$\bar{T} = RT_{d0}(R)/R_d, \kappa_0 = k/(c_p R_d^2), \lambda_n \text{ are solutions to the equation:}$$

$$\lambda_n \cos \lambda_n + h_0 \sin \lambda_n = 0,$$

$$h_0 = \frac{hr_d}{k_l} - 1, \|V_n\|^2 = 0.5(1 - \sin 2\lambda_n / 2\lambda_n),$$

$$V_n = \sin(\lambda_n R / R_d),$$

$$p_n = \frac{1}{\|V_n\|^2} \int_0^1 \left[ \frac{RP(t, R)}{R_d} \right] V_n(R) d(R/R_d).$$

The value of  $h$  was estimated based on the Nusselt number. When estimating the latter, the following correlation was used [1,9]:

$$Nu = 2 \frac{\ln(1 + B_T)}{B_T} (1 + [(1 + Re_d Pr_d)^{1/3} \max[1, Re_d^{0.077}] - 1] / [2F(B_T)]), \quad (8)$$

where  $B_T$  is the Spalding heat transfer number,  $Re_d$  and  $Pr_d$  are Reynolds (based on droplet diameter) and Prandtl numbers respectively,

$$F_T = (1 + B_T)^{0.7} \frac{\ln(1 + B_T)}{B_T}. \quad (9)$$

Solution (7) was implemented into the numerical code, taking into account the changes of gas temperature at each time step. The distribution of temperature inside the droplet at the beginning of the time step was used as the initial condition for Solution (7). This solution was used as the initial condition for the following time step.

### Configuration

The solution was carried out in a three dimensional rectangular domain (128x128x512 mesh) with free boundaries everywhere. The heating of a single mono-component n-dodecane droplet is studied for a certain range of Peclet numbers corresponding to velocity range 0.1 m/s – 1 m/s.

The droplet initial temperature is 350 K and the ambient gas temperature is fixed at 800 K. Ambient pressure is 30 bar. The droplet initial diameter is 100  $\mu\text{m}$ . Velocities and dimensionless parameters used in the analysis are presented in Table 1. The same physical properties are used in DNS and modelling. The simulation is stopped when the droplet reaches the region close to the end of the domain.

In the DNS case, the droplet decelerates due to shear stress between gas and liquid. Hence, at the final time step velocities are decreased by 15-25% depending on the case studied. This leads to a corresponding decrease in the values of Reynolds and Peclet numbers. In the modelling approach, this decrease in  $U_d$  was ignored at this stage.

$U_d$	$Re_d$	$Pe_d$	$Pr_d$
0.1	11.5	143	12.51
0.2	23	286	
0.4	46	572	
0.6	68.5	857.5	
1	106.5	1332	

**Table 1.** Velocities and dimensionless parameters used in this study.

## Results and Discussion

DNS results for three velocities are shown on Figures 1 and 2 for the regions outside and inside the droplet. The influence of the droplet velocity can be clearly seen in both Figures. As follows from Figure 1, the temperature plume is greater when the velocity is higher. The temperature gradient in front of the droplet is high whereas that behind the droplet is low.

As to the temperature gradient inside the liquid phase (see Figure 2), it can be seen that vortex structures do not have enough time to develop during the simulation process. The quasi-steady state has not been reached in the cases studied at the present stage. We have noticed that this stage is difficult to reach, mainly due to the computational cost required. At the same time, most models used in engineering applications are based on the quasi-steady state assumption and do not describe the transient heating properly.

DNS can predict the mean droplet surface temperature  $T_s$ , and average liquid temperature  $T_{avg}$ . The temporal evolution of these two temperatures is shown in Figures 3 and 4. As expected, both these temperatures increase with time. For low velocities, the surface temperatures increase more slowly than for high velocities, in agreement with the prediction of Equation (8).

As one can see from these figures, the higher the velocity, the higher the surface temperature, as expected. However, for the 1 m/s case, at the end of the simulation the surface temperature appears to be less than the one obtained at 0.6 m/s. This behaviour can be attributed to the fact that the increase in the surface temperature for fast moving droplets reduced the amount of heat spent on droplet heating (the difference between gas and droplet surface temperatures decreases). Similarly to the surface temperature, liquid average temperature increases faster for high velocity cases than for low velocity cases. In contrast to the surface temperatures, liquid average temperatures do not have a tendency to merge for different velocities at the end of the simulation.

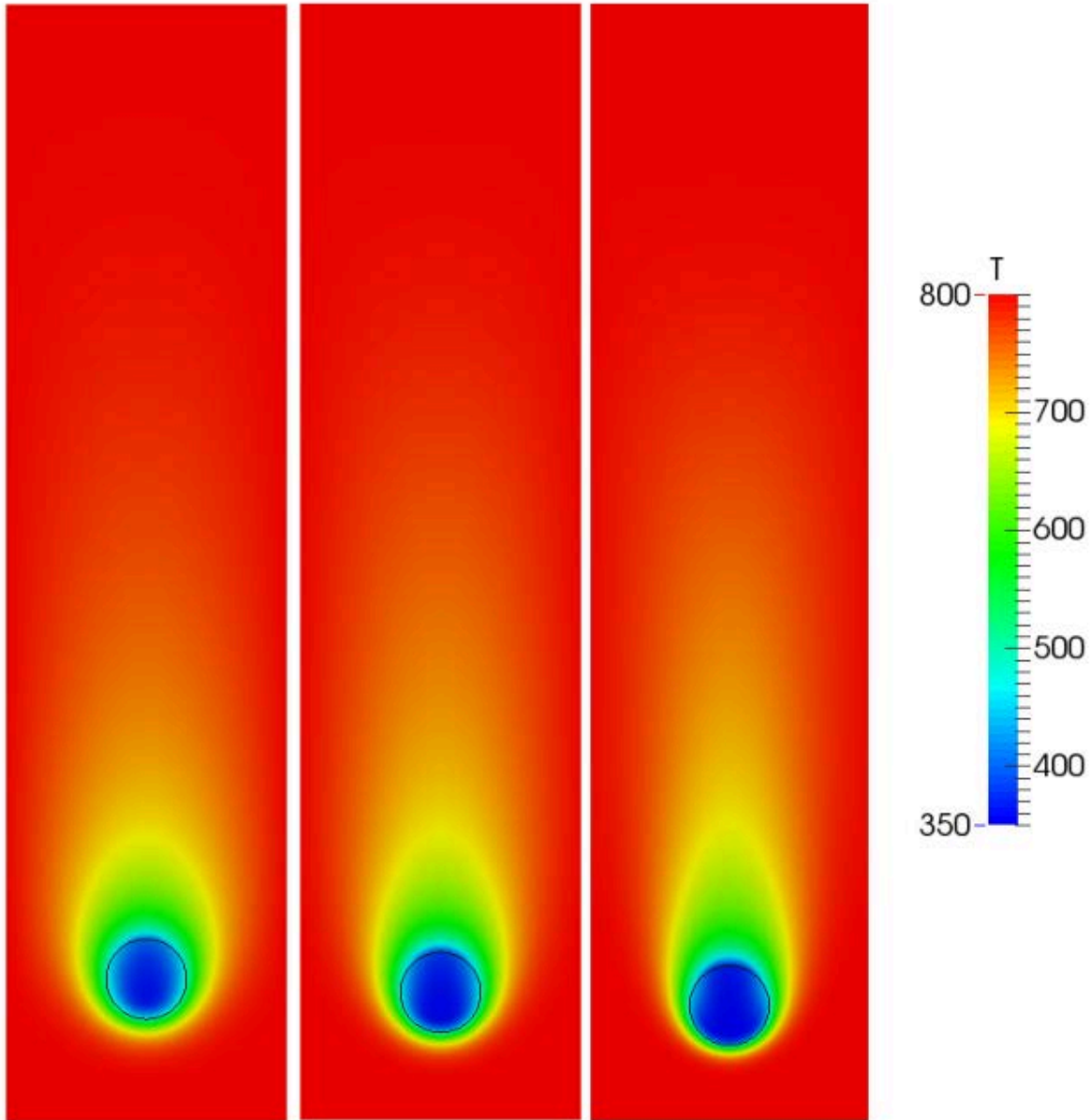


**Figure 1.** 2D visualization of the temperature distribution around the droplet at the final stage of the simulation. From left to right:  $U_f=0.4$  m/s, 0.6 m/s and 1 m/s.

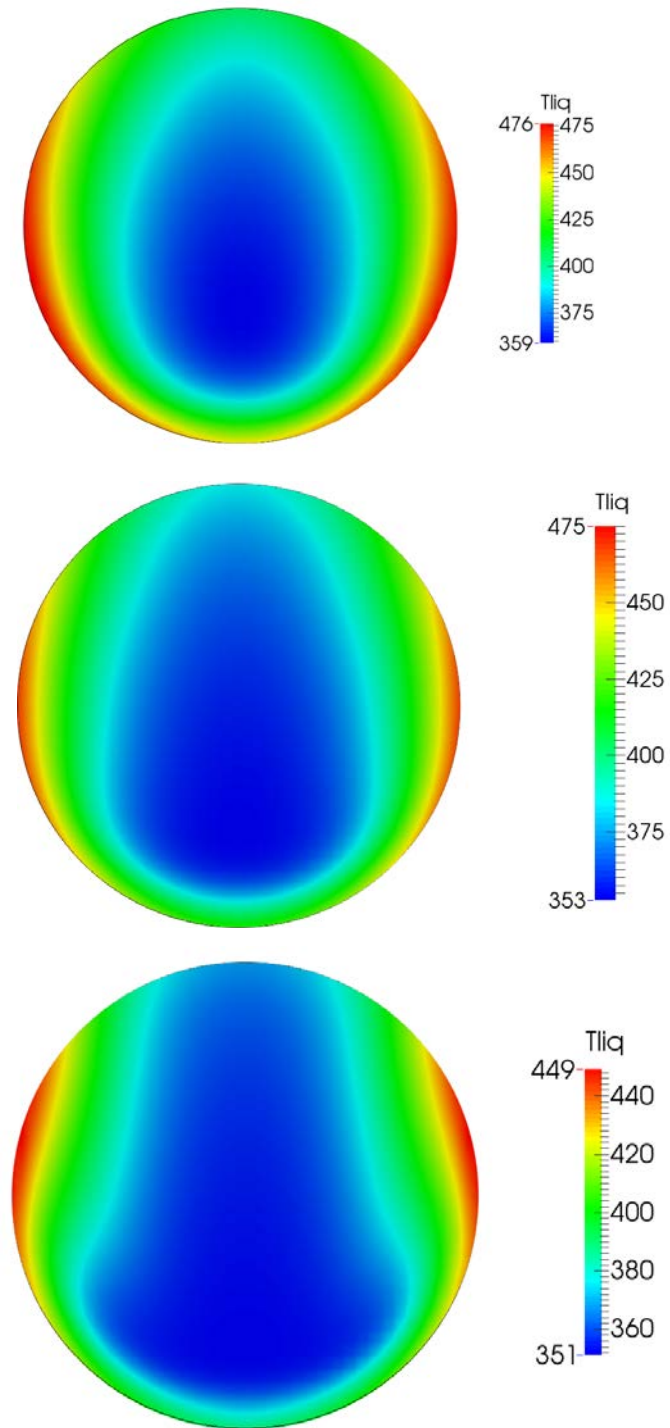


**Figure 2.** 2D visualization of the temperature distribution inside the droplet for  $U_d=0.4$  m/s, 0.6 and 1 m/s (from top to bottom) at the end of the simulation.

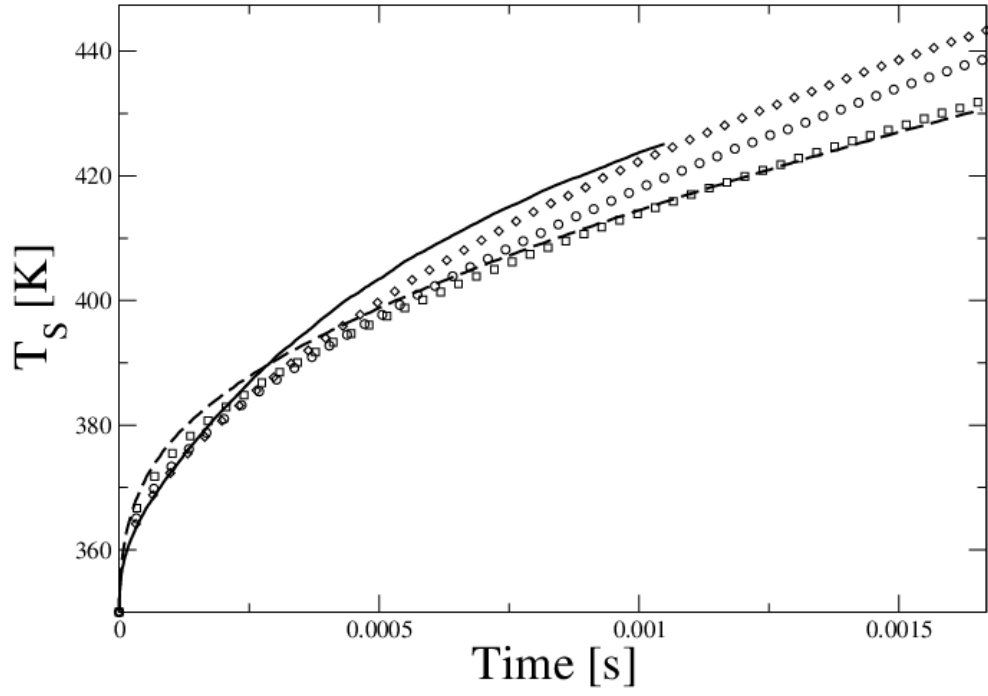


**Figure 3.** Temporal evolution of the averaged surface droplet temperature. Solid: 1 m/s, dotted: 0.1 m/s,  $\square$ : 0.2 m/s,  $\circ$ : 0.4 m/s, and  $\diamond$ : 0.6 m/s.

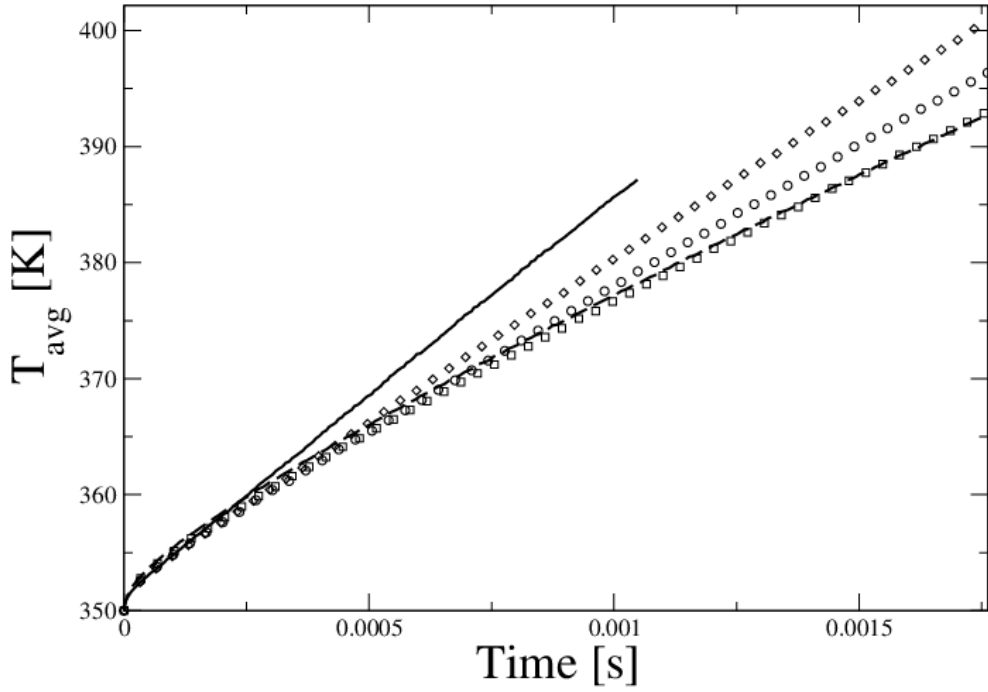


**Figure 4.** Temporal evolution of the average droplet temperature. Solid: 1 m/s, dotted: 0.1 m/s,  $\square$ : 0.2 m/s,  $\circ$ : 0.4 m/s, and  $\diamond$ : 0.6 m/s.

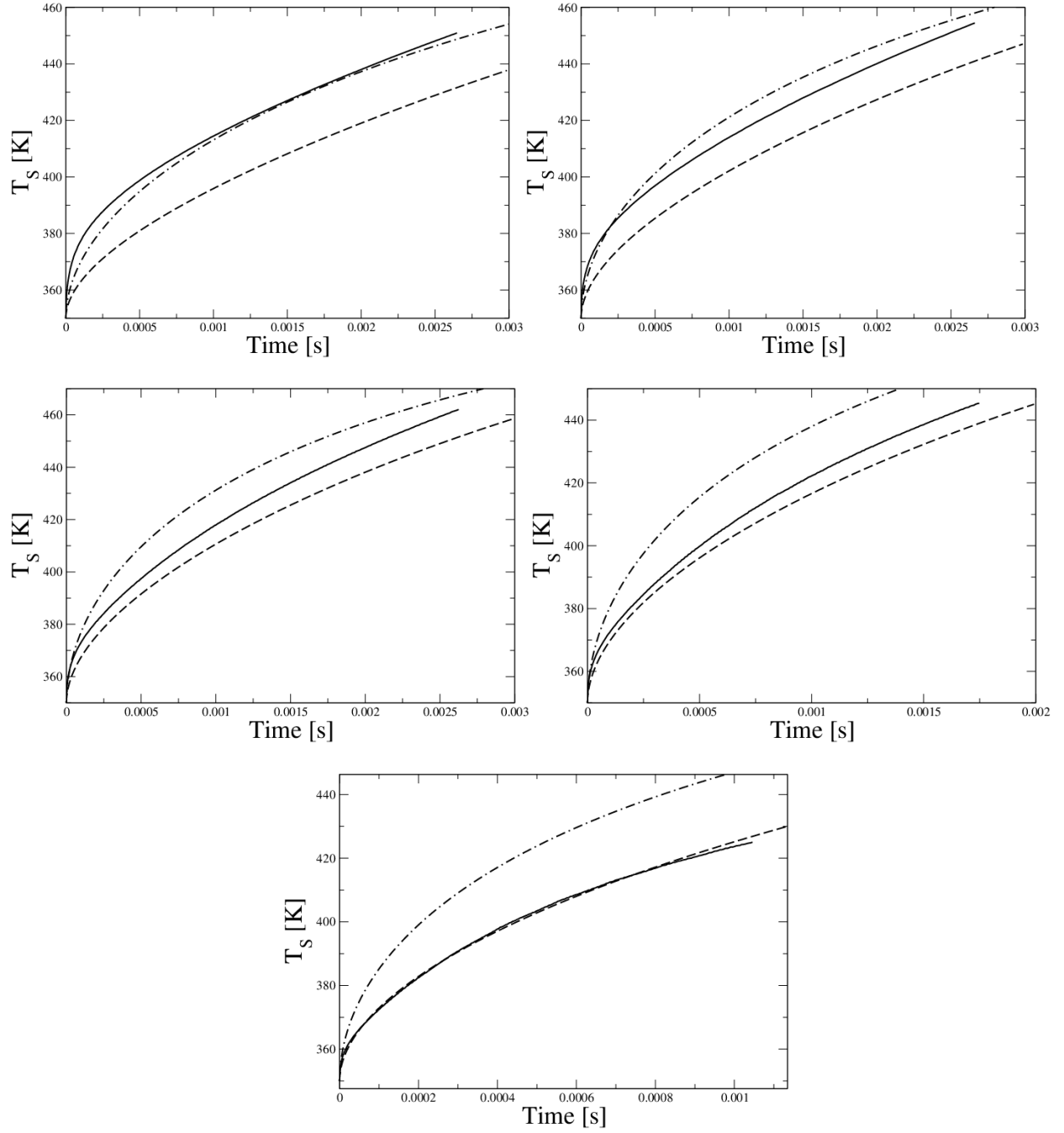


**Figure 5.** Temporal evolution of the averaged surface droplet temperature for 0.1 ms, 0.2 m/s, 0.4 m/s, 0.6 m/s and 1 m/s (from left to right, and top to bottom). Solid: DNS results, dashed: modelling results using  $\lambda_{eff}$ , dashed-dotted: modelling results using  $\lambda_l$ .

The results of comparison between DNS and the modelling approaches are presented in Figure 5 for velocities 0.1 m/s to 1 m/s assuming that liquid thermal conductivities are equal to  $\lambda_{eff}$  (the effect of recirculation is taken into account) and  $\lambda_l$  (the effect of recirculation is ignored). As one can see from Figure 5, for low initial velocity cases the predictions of the model based on  $\lambda_{eff}$  are visibly different from the predictions of the DNS. However, when the initial velocity is increased, modelling results almost perfectly match the DNS curve. For low velocity cases, the use of  $\lambda_l$



gives a better agreement with DNS results. DNS results are effectively bounded by the two modelling curves in every case, except for 0.1 m/s.

These results show the strong impact of the liquid thermal conductivity used in the modelling approach, even for a simple configuration such as a convectively heated spherical droplet. Moreover, since the physical properties remain constant, the Prandtl number remains constant during the simulation.

The correction factor  $\chi$  is close to 2.7 in each case (it varies from 2.72 to 2.64). For the case under consideration, one can conjecture that the correction factor is overestimated for Peclet numbers between 142 and 857 although further investigation of this effect is required. Improvements might be needed for the correlation for  $\chi$  which can be recommended for engineering applications. These preliminary results, however, need to be treated with caution as the quasi-stationary state has not been reached in DNS at the present stage, and the database could be improved by doing more computations in this specific Peclet number range.

In the case of stationary droplets our DNS results with a temperature jump at the interface were compared with the predictions of the transient model developed in [10,11]. Almost perfect agreement for the predicted droplet surface temperatures was achieved. At the same time DNS results, in which a realistic initial distribution of temperature in the gas phase was used, appeared to be close to the ones predicted by the model based on Equations (7) and (8). Which initial distribution of temperature should be used in DNS to allow meaningful comparison between DNS and modelling results is still an open question.

## **Conclusion**

A preliminary comparison between DNS and modelling results for a typical n-dodecane droplet heated without evaporation in a hot gas are presented. DNS of two-phase flows allows us to solve the heat transfer equation in both phases and at the interface. The classical modelling approach, suggested by Abramzon and Sirignano, supplemented by the analytical solution to the heat transfer equation inside droplets, was used in our analysis. Effects of recirculation inside moving droplets were taken into account using the effective thermal conductivity (ETC) model. A moving droplet configuration was set up and a database was created to study the heating process for various Peclet numbers.

The results show that the predictions of the model are rather different from the predictions of DNS for the heating process in relatively low velocity cases. However, a good agreement between DNS and modelling results is demonstrated for relatively higher velocity cases.

## **Acknowledgments**

The authors are grateful to the EPSRC (Grant EP/K020528/1) for financial support of the work on this project, BP for permission to use their computational resources and CORIA (University of Rouen) colleagues (T. Menard and his team) who allowed the authors to use ARCHER code at the University of Brighton.

## **References**

- [1] Sazhin, S.S., 2014, "Droplets and Sprays".
- [2] Menard, T. et al., 2007, *International Journal of Multiphase Flow*, 33(5), pp. 510-524.
- [3] Tanguy S. et al., 2007, *Journal of Computational Physics*, 221(2), pp. 837-853.
- [4] Duret, B. et al., 2013, *International Journal of Multiphase Flow*, 55(0), pp. 130-137.
- [5] Abramzon, B. and Sirignano, W.A., 1989, *International Journal of Heat and Mass Transfer*, 32, pp. 1605- 18.
- [6] Aslam, T., 2004, *Journal of Computational Physics*, 193(1), pp. 349-355.
- [7] Duret, B., 2013, *Simulation numérique directe des écoulements liquid-gaz avec évaporation: application à l'atomisation*, PhD thesis, University of Rouen.
- [8] Duret, B. et al., 2013, 8th International Conference on Multiphase Flow (ICMF), Jeju, Korea.
- [9] Sazhin, S.S., 2014, *Fuel*, 129, pp. 238-266.
- [10] Sazhin, S.S. et al., 2007, *International Journal of Thermal Sciences* 46, pp. 444-457.
- [11] Sazhin, S.S. et al., 2011, *International Journal of Thermal Sciences* 50, pp. 1215-1222.